α5β1 Integrin Mediates Pulmonary Epithelial Cyst Formation

Susan K. Legan[1], **Daniel D. Lee**[2], and **Margaret A. Schwarz**[2]

[1]Department of Pediatrics, University of Texas Southwestern Medical Center at Dallas

[2]Department of Pediatrics, Indiana University

Abstract

Background—Formation of the epithelial cyst involves the establishment of apical – basolateral polarity through a series of cellular interactions that are in part mediated by the extracellular matrix (ECM). We report that in a three-dimensional multi-cellular self-assembly model of lung development, α5 integrin regulates epithelial cyst formation through organization of soluble fibronectin matrix into insoluble fibrils through a process called fibrillogenesis.

Results—Dissociated murine embryonic lung cells self-assemble into three-dimensional pulmonary bodies that are dependent on α5β1 integrin mediated fibrillogenesis for cell-cell mediated self-assembly - compaction and epithelial cyst formation. Knockdown of *a5* integrin resulted in a significant increase in another mediator of fibrillogenesis, αV integrin. Compensatory increased expression of another mediator of fibrillogenesis, αV integrin, was not sufficient to normalize epithelial cyst formation. Loss of α5 integrin-mediated fibrillogenesis perturbed the ability of clustered epithelial cells to establish clear polarity, loss of epithelial cell pyramidal shape, and disrupted apical F-actin-rich deposition. Lack of rich central epithelial localization of F-actin cytoskeleton and podocalyxin suggests that loss of α5 integrin-mediated fibrillogenesis interferes with the normal cytoskeleton organization that facilitates epithelial cysts polarization.

Conclusion—We conclude that lung epithelial cyst formation in development is mediated in part by α5β1 integrin dependent fibrillogenesis.

Keywords

alveolar; lung development; pulmonary bodies; epithelial cyst

Introduction

During pulmonary development, mechanical forces created by living cells are essential to cellular orientation and organogenesis. Fundamental to cellular initiated mechanical forces, cells establish and manipulate their environment through the secretion of an extracellular

matrix (ECM) that facilitates the structural organization of cellular components within the distal lung into an alveolar and vascular interface capable of oxygen exchange.

Integrins are Type I transmembrane proteins composed of two noncovalently linked alpha (α) and beta (β) subunits that designate ligand-binding specificity (Legate et al., 2009). Expressed as eighteen α subunits and eight β subunits, 24 different combinations with overlapping cell-type expression patterns and substrate specificity are formed (Hynes, 2002). However, it is the specific pairing of the individual α and β integrin subunits expressed by the cell type that dictates which extracellular matrix (ECM) the cell can bind to. Fibronectin (FN), a multifunctional adhesive glycoprotein, is a prolific ECM protein that is essential for normal development (Hynes, 1990). Secreted as a disulfide-bonded dimer, it binds principally to integrin cell surface receptors. Binding of FN to its integrin receptor initiates the unfolding of this soluble protein, followed by its assembly into a detergent insoluble fibrillar matrix (fibrillogenesis). This insoluble form of FN includes a component of the ECM that can modulate both cell behavior and tissue cytoskeleton architecture. FN protein diversity occurs due to alternative splicing of two type III exons referred to as Extra Domains (ED) A and B with EDA FN being predominately associated with lung fibrosis following injury (White and Muro, 2011). Several integrin receptors bind to FN to facilitate cell adhesion and migration. These include the β1 integrins, α5β1, α4β1, α8β1 and αVβ1 (Akiyama et al., 1989, Schnapp et al., 1995, Yang et al., 1993). However, the specialized process of FN fibrillogenesis is largely confined to the α5β1 integrin (Mao and Schwarzbauer, 2005, Wierzbicka-Patynowski and Schwarzbauer, 2003).

Alpha5Beta1 integrin, a member of the heterodimeric transmembrane glycoprotein family, exhibits specificity for the ECM ligand fibronectin (FN) via an RGD binding site. Binding of α5β1 to its ligand initiates a complex of downstream signaling events resulting in cellular reorganization of the actin cytoskeleton that facilitates cell migration and assembly of a three-dimensional (3-D) fibrillar matrix (fibrillogenesis) (Robinson et al., 2004, Robinson et al., 2003). In contrast to the known role of α5β1 in angiogenesis, the role of α5β1 in epithelial cell regulation and pulmonary morphogenesis is unknown. The importance of this FN fibrillogenesis is supported by the fact that genetic ablation of α5β1 integrin results in major vascular abnormalities and leads to early embryonic fatality (Francis et al., 2002, Hynes, 2002, Taverna and Hynes, 2001) although single deletion of either the EDA or EDB domains results in a viable mouse suggesting that both domains are not critical or that other proteins are able to compensate for a specific isoform (Fukuda et al., 2002) (White and Muro, 2011). In contrast, genetic manipulation of αVβ3 and αVβ5 integrins indicate that the αV integrin / FN interactions are not necessary for vascular formation (Hynes, 2002). During pulmonary morphogenesis, α5β1 integrin and its ECM ligand FN are expressed during lung development (Chen et al., 1986, Roman and McDonald, 1992, Snyder et al., 1987) and have been shown to be essential for lung branching morphogenesis (Sakai et al., 2003) (Plosa et al., 2014).

Although the factors affecting α5β1-mediated adhesion to FN have been examined, surprisingly little is known regarding the contribution of the mechanical forces generated by integrin mediated FN – fibril formation on pulmonary tissue complexity and functional formation. Limited by embryonic lethality due to loss of α5, our studies utilize the well-

defined model of lung self-assembly that has the unique capacity of de novo three-dimensional re-assembly (Schwarz et al., 2011). We determined that α5 mediated fibrillogenesis modulates fetal lung cellular self-organization and self-assembly. In conjunction with a reduction in fibrillogenesis, a compensatory increase in another mediator of fibrillogenesis, αV integrin was not sufficient to rescue self-assembly, fibrillogenesis, or normalize epithelial cyst formation. Examination of epithelial polarity determined that closed epithelial cysts demonstrate a front-rear polarity. Importantly, our studies indicate that α5 mediated fibrillogenesis is important for normal pulmonary epithelial cyst formation in the developing lung as inhibition reduces epithelial cyst size and subsequent perturbation of epithelial polarity.

Results

Alpha5 Beta1 integrin is an abundant cell membrane receptor in fetal pulmonary cells that modulates aggregate compaction

Dissociated multi-cellular fetal lung has the unique capacity to spontaneously self-assemble de novo in three-dimension (3D) hanging drops (HD) (Schwarz et al., 2011). Previous studies implicate adhesion-based mechanisms in single cell population as well as multi-cell lung aggregation and self-assembly through inhibition of the extracellular matrix deposition of the glycoprotein FN fibrillogenesis (Robinson et al., 2003, Schwarz et al., 2011, Mao and Schwarzbauer, 2005, Wierzbicka-Patynowski and Schwarzbauer, 2003). Flow cytometry indicates cell surface expression of α5 and β1 in the fetal lung cell population (Figure 1A). In 3D, HD fetal lung cells spontaneously rearrange into spheres allowing individual cell populations to maximize their mutual bonding and minimize adhesive free energy (Foty et al., 1994, Foty et al., 1996, Foty and Steinberg, 2005, Robinson et al., 2003, Steinberg, 1962, Schwarz et al., 2011). Aggregation or compaction, a function of cellular rearrangement over time, was assessed at 48 hours in 3D HD. HDs treated with an α5-neutralizing antibody were significantly larger at 48 hours consistent with less compaction or self-assembly than those HDs treated with non-specific IgG (Fig. 1B). Concurrent with α5β1 neutralization, there was a loss of FN matrix assembly, noted by a reduction in insoluble FN (Fig. 1C,D) and deposition of short punctate insoluble FN strands (Fig. 1F: arrows) as compared to long continuous FN strands found in non-specific IgG (Fig. 1E: arrows).

Knockdown of Alpha5 integrin decreases HD aggregation

Cell-cell interactions mediate lung formation. 3D HD function as a surrogate to assess α5β1-integrin impact on tissue properties. In this dynamic model, dictated by intercellular connections, a cell's ability to communicate effectively with neighboring cells results in a quantifiable sphere formation known as compaction. Compaction or cell aggregation was assessed after 48hr in HD. Knockdown of α5 inhibited lung compaction, as HDs were significantly larger at 48hr suggesting that self-assembly was decreased as compared to Scrambled siRNA (Fig. 2A). Knockdown of α5 protein levels was confirmed by Western blot analysis (Fig. 2B).

Knockdown of Alpha5 disrupts FN matrix assembly

Fibronectin matrix assembly not only mediates cell-cell interactions in a mixed cell population, it has also been shown to be an important regulator of aggregate cohesion and is directly mediated by α5β1 integrin. At baseline, HDs demonstrate fibrillogenesis noted by deposition of insoluble FN in long strands within the HD (Fig. 3B: stars) as well as at the epithelial/mesenchymal interface (Fig. 3A: dotted outline). In contrast, lung HDs treated with *Itga5* siRNA had a notable reduction in insoluble FN fibrils. Furthermore, the FN fibrils that were present exhibited different characteristics. In contrast to long strands, the FN depositions were thick, small arrowhead / punctate like (Fig. 3C,D: arrows). Insoluble deposited FN (DOC fraction), soluble, and as different splice variants (EDA vs EDB), FN protein and solubility was examined. DOC isolation of FN supported a reduction in insoluble FN (Fig. 3E,F) and total FN protein (Fig. 3E,G) with a reduction in the alternative splice variants EDA in the *Itga5* siRNA while the EDB was unaffected as compared to Scrambled siRNA (Fig. 3E). Importantly, qPCR analysis determined overall FN transcription was not inhibited by *Itga5* siRNA (data not shown).

Lung epithelial cyst size and basement membrane proteins laminin and vitronectin localization are altered by knockdown of Alpha5

Cytoskeleton organization is a fundamental component of distal pulmonary epithelial cell lumen formation; however little is know regarding the role of FN matrix assembly in lumen formation. Supportive of an important role for FN-dependent architecture in lung development is the observation that although protein levels of the ECM total laminin were similar (data not shown), histological analysis revealed that basilar epithelial deposition of laminin was discontinuous and pyknotic in cysts treated with *Itga5* siRNA (Fig. 4B,D: arrows) as compared to scrambled siRNA (Fig. 4A,C: stars). Laminin, found at the epithelial / mesenchymal interface during normal lung development (Schuger, 1997, Schuger et al., 1992), was noted to be distributed in a similar location in the 3D HD pulmonary sheets. Using this established marker of the epithelial / mesenchymal border, epithelial cyst diameter was defined by its laminin basement membrane border. Examination of *Itga5* siRNA epithelial cysts revealed a less complex cyst formation and reduction in cyst size (Fig. 4B,E) as compared to Scrambled siRNA (Fig. 4A,E). In contrast to reports associating selective apoptosis with expanding lumens (Debnath et al., 2002), we observed a significant increase in epithelial cell proliferation as evidenced by increased Ki67 counts in *Itga5* siRNA HD (Fig. 5) as compared to Scrambled siRNA. Despite the increase in epithelial cell proliferation, within the predominant epithelial cell population at this age, surfactant protein C (SPC) expression, a marker of type II epithelial cells, was not significantly impacted (data not shown). Examination of other matrix components by Western blotting indicated a concomitant reduction in vitronectin (Fig. 4F,G) and compensatory increase in AlphaV integrin (Fig. 4H,I).

Lung epithelial cyst formation is mediated by Alpha5 fibrillogenesis

Recent studies observed that loss of lumen formation is associated with disruptions in epithelial polarity (Davis and Cleaver, 2014, Itoh et al., 2007). In conjunction with an observed loss of lumen formation in *Itga5* siRNA reduction, epithelial cell polarity was

examined. Apical polarity of the epithelial lumen in Scrambled siRNA HDs was confirmed by central deposition of Podocalyxin (PODXL) (Fig. 6A,B: arrow) while a lack of central distribution of PODXL in *Itga5* siRNA HDs suggested an alteration in apical-basolateral polarity (Fig. 6A,B: star). This is further supported by co-localization of E-cadherin with F-actin where pyramidal epithelial cells with F-actin-rich central deposition defined epithelial lumen formation in Scrambled siRNA (Fig. 6B,C: arrow). Epithelial pyramidal cell shape is guided by actin-rich apical deposition. In contrast, *Itga5* siRNA epithelial cysts demonstrated more columnar shaped epithelial cells, F-actin-poor central lumen deposition (Fig. 6B,C: star) and discontinuous E-cadherin deposition consistent with disrupted adherens junctions (Fig. 6C: dotted line). Lack of pyramidal shaped epithelial cell and F-actin-poor deposition in *Itga5* siRNA HDs was associated with reduction in polarity markers NUMB and PODXL (Fig. 6A,B,D). Scrambled siRNA HDs where closed lumens demonstrate pyramidal shaped epithelial cells and front-rear NUMB expression (Fig. 6D: arrow indicates strong rear expression and star indicates lessened front expression), *Itga5* siRNA lumens lacked apical or basolateral NUMB expression (Fig. 6D).

Discussion

Here, we elucidate that α5β1 integrin mediated fibrillogenesis is a moderator of epithelial cyst formation and polarity. Initially, blockade of α5β1 inhibited fibrillogenesis and delayed lung self-assembly. Consistent with previous reports in single cell populations where knockdown of α5β1 integrin redistributed focal adhesions and contractile shape (Huveneers et al., 2008), we show that in 3D HDs α5 knockdown was sufficient to delay lung self-assembly. Concomitant with α5 knockdown, there was loss of insoluble FN organization - fibrillogenesis, F-actin-poor central epithelial lumen deposition, disrupted epithelial front-rear polarity, concurrent reduction of both cyst formation and abutment of the PODXL at the epithelial apical surface. Collectively, these studies support a role for α5β1 mediated FN dependent fibrillogenesis in epithelial polarity and lumen formation in the developing lung.

Pulmonary organogenesis requires a tightly controlled series of events that result from specific cell – cell and cell – extracellular matrix (ECM) interactions with their environment. Importantly, not only do cellular interactions influence their environment, but also cells are also actively involved in the creation of their environment. In concert with multiple growth factors (Cardoso, 2001, Cardoso and Lu, 2006, Warburton and Lee, 1999), cells secrete and manipulate ECM components into suitable configurations that sustain and facilitate the organization of the alveolar/vascular cell interface resulting in a functional air-exchanging lung. Optimization of these micro-environmental cues is necessary in the assembly of a functional pulmonary unit. The ECM matrix is composed of two main types: (1) the interstitial connective tissue matrix that surrounds the cells providing a structural scaffold and (2) the basement membrane that separates the epithelium from the surrounding stroma that is responsible for controlling cell organization (Bonnans et al., 2014). Previous studies demonstrate the importance of the basement membrane matrix in orientation of epithelial cell polarity. In single-cell type kidney epithelial cysts, Rac1-mediated laminin assembly regulated apical pole orientation within the cyst and ensured the coordination of polarity (O'Brien et al., 2001). Furthermore, inhibition of β1 integrin (Yu et al., 2005) or Rac1 (O'Brien et al., 2001) prevented the organization of laminin within the basement membrane

resulting in polarity inversion. In our studies, although total laminin protein levels were unchanged, *Itga5* siRNA altered laminin deposition where it was noted to be discontinuous and pyknotic. In contrast to laminin being part of the basement membrane component of the ECM, FN is a member of the interstitial connective tissue matrix that contributes to the structural scaffolding. In our studies, disruption of the interstitial connective matrix component FN not only altered the deposition of the basement matrix component laminin, but it also directly impacted the structure and polarity of the epithelial lumen as manifested by loss of epithelial cell pyramidal shape, central F-actin-poor epithelial lumen expression, and altered distribution of the polarity markers NUMB and PODXL. F-actin alignment is regulated by FN binding to α5β1 integrin. Knockdown of α5 integrin decreases F-actin cytoskeleton organization. Loss of the adhesive strength provided by the central F-actin-rich bundles implies that the actin-based cytoskeleton used for the attachment of cell adhesion proteins is altered (Wan et al., 2013). This is supported by our findings that E-cadherin deposition is discontinuous in the *Itga5* siRNA HD. Importantly, elevation of an alternative director of fibrillogenesis, αV integrin, was not able to completely rescue epithelial cyst formation. Taken together, these findings suggest that factors effecting epithelial polarity are not limited to the basement membrane matrix, but rather that the basement membrane and interstitial connective tissue matrix work in concert with the cells cytoskeleton to influence epithelial polarity and cyst formation.

Fibrillogenesis, mediated by α5β1 is responsible for cell behavior and tissue architecture (Robinson et al., 2004, Robinson et al., 2003). FN assembly is mediated by an RGD binding motif through either α5β1 or αV integrins receptors. Previous *in vivo* and *in vitro* studies have determined that despite binding FN via a similar RGD binding motif, differing receptors α5β1 and αV integrins are activated with the downstream signaling and assembly of FN fibrils being independent of each other. As a result, αV mediated FN assembly is less dense and contains thicker and shorter fibrils with arrowhead-like focal adhesions while, α5β1 assembled fibrils are thin and long (Takahashi et al., 2007). Examination of the FN fibrils deposited in the α5 knockdown HDs found them to be short, thick and arrowhead-like. These fibrils are typical of αV mediated FN fibril assembly. Elevated protein levels of αV integrin in *Itga5* siRNA HDs not only support the focal adhesion deposition pattern, but also suggest a compensatory increase. Interestingly, αVβ3's affinity for FN isoforms is different from that of α5β1 integrin. A recent study determined that αVβ3 integrin has a marked affinity for EDB fibronectin that is greater than its affinity for plasma FN (Kraft et al., 2016). This in part could explain a noted reduction in EDA FN in *Itga5* siRNA HD that express a compensatory increase in αVβ3 integrin. One possibility is that there are different but complementary roles that αV versus α5β1 integrin mediated fibrillogenesis supports. The thicker and shorter αV-mediated fibrils with arrowhead-like focal adhesions could function as extracellular matrix anchors that are then spanned by α5β1 integrin mediated long thin FN fibrils. In this cooperative state, FN fibrillogenesis becomes a sequential anchored network formed by bridging. Loss of the fine connecting α5β1-mediated fibrils results in increased αV mediated fibrils that cannot structurally compensate for the loss of the spanning connector fibrils. Loss of this structural network results in a collapse of cytoskeleton integrity. This is further supported by recent findings that not all FN fibrillar networks provide the same cytoskeleton support as cytoskeleton tension and adhesion

complex maturation is dependent on this α5β1 mediated fibril assembly (Danen et al., 2002). We speculate that loss of the spanning connector fibrils has greater implications that reach beyond epithelial cyst formation. For example, previous studies in submandibular and mammary gland ductal elongation and branching have been directly associated with ECM remodeling (Bonnans et al., 2014). Future studies will explore the impact that α5 mediated fibrillogenesis has on lung branching during development.

Previous studies determined that loss of the ECM and β1 integrin negatively impacts lung branching during development. Plosa et al. established that epithelial β1 integrin was required throughout the different stages of lung development for airway branching morphogenesis, alveolarization, and maintenance of homeostasis (Plosa et al., 2014). However, the mechanisms of how epithelial branching and factors contributing to alveolar lumen structural formation have not been determined. The alveolar lumen is multi-cellular and predominately composed of air-exchanging alveolar type 1 cells and surfactant producing alveolar type 2 cells supported in part by an extracellular matrix that abut the endothelium. Epithelial lumen formation is dependent on the integrity and adhesive strength of the cytoskeleton actin bundles and apical-basolateral polarization of cells. Recent studies determined that the ECM-signaling is essential in reorienting cell polarity. In these studies, when Podocalyxin (PODXL) abuts the extra-cellular matrix, polarity is inverted (O'Brien et al., 2001). In single cell canine kidney epithelial cells grown in 3D matrigel, reorientation of cell polarity from basilar to apical location results in lumen formation, and is dependent on the conversion of a non-polar cell population to an apical-basolateral polarized cyst. Suppression of the α2β1 or α3β1-integrin signaling promotes the apical relocalization of the PODXL/NHERF1/Ezrin complex, resulting in removal of ECM-abutting PODXL and initiation of its transcytosis to the apical membrane where it initiates epithelial inversion of polarity, and lumen formation occurs. These studies support the concept that blockade of PODXL mobilization from the ECM results in an epithelial cyst that demonstrates a collective front-rear polarity that lack lumen formation (Bryant et al., 2014, Davis and Cleaver, 2014).

We found that there was a loss of central F-actin-rich deposition in epithelial lumens upon *Itga5* siRNA knockdown, which we denote here as 'F-actin-poor-region.' Associated with the F-actin–poor region, there is also a loss of central podocalyxin (PODXL). Previous reports show PODXL either in basilar or apical location (O'Brien et al., 2001, Bryant et al., 2014, Davis and Cleaver, 2014). Similarly, in control PBs, we found that PODXL was also both apical and found to be located within the center of the F-actin-rich region. However, loss of α5 integrin-mediated fibrillogenesis did not place PODXL at either the apical or basilar region. Rather it co-localized with the F-actin-poor region. In conjunction with the *Itga5* siRNA F-actin-poor region, there was also notable discontinuous deposition of E-cadherin. During lumen formation, F-actin is organized through self-alignment following binding of α5β1 integrin to FN. Loss of this interaction would decrease F-actin organization. Actin-based cytoskeleton is important for the attachment of cell adhesion proteins such as E-cadherin. Therefore, loss of α5 disrupts alignment of F-actin, its binding to adhesion proteins, and its ability to traffic actin mediated polarity proteins. Furthermore, epithelial lumen cells with loss of apical concentration of F-actin, were more likely to have a columnar shape and not the typical pyramid shape found in actin-rich lumens. Analysis of

polarity markers NUMB and PODXL supports a disruption of polarity in *Itga5* siRNA HDs. Lastly, lack of basilar or apical PODXL distribution suggests that PODXL is disrupted from the ECM membrane but lacks engagement of its transport system to the cells' apex. Our findings are consistent with previous observations where β1 blockage disrupted alveolar type II cell cyst formation (Yu et al., 2007) where single cell populations failed to form epithelial cyst. Our findings examine the role of specific α5β1 in a multi-dimensional HD where epithelial cyst formation occurred, but demonstrate perturbed polarity. These findings likely are a direct result of compensatory measures that facilitate epithelial cyst formation but cannot compensate for the fibrillogenesis contributions that α5β1 provides to epithelial lumen polarity. However, not all factors that regulate cell polarity were examined in these studies. For example, pseudokinase ILK signaling has also been described mammary epithelial cell polarity (Akhtar and Streuli, 2013). Furthermore, polarity and lumen formation occurs over a prolonged period and involves factors not examined here such as vascular formation and epithelial cell differentiation. Therefore other factors are likely to be involved in the process of epithelial cyst formation.

Conclusions

Based on our collective findings, α5 integrin is identified as being a critical factor in lung epithelial lumen polarity, cohesion of assembled lung, and a contributor to alveolar cyst formation. Previous studies determined that α5β1 is essential for embryonic vessel formation and viability (Francis et al., 2002, Hynes, 2002, Taverna and Hynes, 2001). Using a model of lung self-assembly, we show that *α5* integrin contributes to lung epithelial polarity and cyst formation as blockade or knockdown of α5 perturbed epithelial polarity and cyst formation. However, despite slowing lung self-assembly, HD formation is not dependent on α5 mediated fibrillogenesis. These findings suggest a targeted role in α5 signaling for which compensation in fibrillogenesis through other mechanisms such as αV is not sufficient, mainly epithelial lumen formation and polarity. Although this model of lung self-assembly does not completely replicate lung development, it represents a step forward in determining the role that α5β1 mediated fibrillogenesis has in lung assembly and epithelial cyst formation in the developing lung. Therefore we propose that together these findings suggest that α5 integrin is a regulator for lung epithelial cyst development.

Experimental Procedures

Cell Culture, Compaction Analysis and Hanging Drop (HD) Pulmonary Sheet Formation

Pulmonary sheets were formed as previously described (Schwarz et al., 2011). In brief, fetal lungs were microdissected from embryos of timed pregnant CD1 mice at embryologic (E) 14.5 days. Lungs were first dissociated in 0.5% Collagenase I (Invitrogen, Carlsbad, CA) and 20μg/ml DNase I (Sigma-Aldrich, St. Louis, MO) mixture, red blood cells removed using RBC lysis buffer (Sigma-Aldrich, St. Louis, MO), and the cell suspension was passed through a 100μM filter. The final single cell co-culture was resuspended in MEM supplemented with 20% FBS (fibronectin-depleted) at a concentration of 1×10^7 cells/ml. Viability was noted to be >95% as determined by trypan blue exclusion. Hanging drops of 12.5μl (125,000 cells/HD) were suspended over PBS on the lids of 60 mm Petri dishes.

Compaction of cells during self-assembly for 48 hours was assessed in phase contrast images captured using a 4× objective by outlining the cellular mass and measurement of the entire outline of the HD in pixel number as previously described (Schwarz et al., 2011). Some HDs were treated with α5 integrin function blocking antibody (CD49e Integrin alpha5 chain 0.25-2µg/ml) (BD Pharminogen, 553318) and compared to controls treated with non-specific IgG from (14131,Sigma Aldrich St. Louis, MO). In other experiments, mouse *Itga5* siRNA duplexes and negative universal controls (Invitrogen, Carlsbad, CA) were reverse transfected using the siPORT™NeoFX™ transfection agent as follows: (1) siPORT™ Neo FX ™ transfection agent and siRNA duplexes were diluted separately in OptiMEM (Invitrogen); (2) siRNA complexes (30 nM) pre-incubated in transfection reagent, were added to cells overnight in 20% FBS (Gemini) MEM at a cell concentration of 1.5×10^5 cells/ml. After trypsinization and detachment from the plates, the cells were allowed to self assemble into aggregates for 48 hours. The aggregates were exposed to a second siRNA transfection during pulmonary body formation. Cell aggregates were transferred to 10 mL shaker flask and developed as pulmonary bodies over 48 hours while shaking 130 rpm at 37°C and 5% CO_2 and analyzed for histology.

Flow Cytometry

Dissociated mouse fetal lung cells were suspended in a 2% FBS / PBS solution at a density of 1×10^7 cells / mL. Cells were placed at a dilution of 1×10^6 concentration in a polystyrene tube and exposed to the conjugated primary antibodies alpha5-Phycoerythrin (Abcam, ab33674) or Beta 1-Phycoerythrin (Abcam, ab36219) for 30 minutes on ice with agitation every 10 min. Following incubation cells were pelleted followed by the cell pellet being resuspended in 1 mL PBS / 2% FBS. Flow cytometry was analyzed by the UTSW core facility. Cells incubated with a secondary antibody Hamster PE (Jackson) or PBS alone served as the control population.

Immunoblot Analysis

Cells were lysed on ice using RIPA lysis buffer (25 mM Tris.Cl, pH 7.6, 150 mM NaCl, 1% NP40, 1% DOC, 1% SDS) supplemented with protease inhibitor cocktail (Sigma). Following analysis of protein concentration (Bradford analysis, Biorad), equal amounts of protein loaded, electrophoresed on SDS-PAGE gel, followed by transfer to Immobilon-P membranes, blocked in a casein-based solution and probed with primary antibodies purchased from: Santa Cruz (alpha5 sc10729, polyclonal fibronectin sc-9068 that recognizes all isoforms, vitronectin sc-74484), Millipore (alpha5 Chemicon AB1928, alphaV Chemicon Ab1930, pro-SPC upstate 07-647 or AB3786, Actin MAB1501, GAPDH MAB374), and Abcam (Laminin ab30320). Binding specificity was detected using chemiluminescence substrate (Pierce, Rockford, IL) and XAR-5 film (Eastman Kodak, Rochester, NY). Quantitative analysis was performed using Quantity One software and samples were normalized to actin / GAPDH / tubulin loading controls.

Soluble and insoluble FN was detected as previously described (Schwarz et al., 2011). In brief, samples were lysed in a DOC lysis buffer (2% sodium deoxycholate, 0.02 M Tris-HCl, pH 8.8, 2 mM PMSF, 2 mM EDTA, 2 mM iodoacetic acid, and 2 mM *N*-ethylmaleimide) and lysates were passed through a 26-gauge needle prior to centrifugation. Following

centrifugation, the supernatant containing the DOC-soluble component was analyzed. DOC-insoluble components from the pellet were solubilized using SDS lysis buffer (1% SDS, 25 mM Tris-HCl, pH 8.0, 2 mM PMSF, 2 mM EDTA, 2 mM iodoacetic acid, and 2 mM *N*-ethylmaleimide). Following isolation, the reduced lysates were normalized by BCA protein content and separated by SDS-PAGE gels and probed with an anti-FN antibody (ab6584, AbCam, Ltd., Cambridge, UK). In reducing conditions, the high-molecular-weight FN multimers resolve as a 220-kDa band. Semi-quantitative densitometry was performed as previously described.

Histological Analysis

Pulmonary bodies were embedded and frozen in OCT after fixation in 4% paraformaldehyde and dehydration in 30% sucrose. Five-micron cryosections were cut and mounted on Histogrip treated slides (Zymed). Following permeabilization with 0.1% Triton-X100 and blocking with CAS blocking buffer (Invitrogen), samples were incubated with primary antibodies from Abcam (fibronectin ab23750, laminin ab30320, Ki67 ab15580, Numb ab14140), Novus Biologicals (Podocalyxin MAB1556) and Millipore (pro-SPC 07-647 or AB3786) as per manufacturer's instructions. This was followed by incubation with the appropriate secondary Cy-3 or Alexa-Fluor 488 fluorescent antibody (Chemicon, Temecula, CA and Molecular Probes Invitrogen, Carlsbad, CA, respectively) and slides were mounted using Slow Fade Gold Anti-Fade reagent with DAPI (Invitrogen: S36938). Apoptotic cells were detected using ApopTag® Red *In Situ* Apoptosis Detection Kit (Chemicon International). Samples in polarity studies were de-identified, randomized and images captured. Following analysis samples were identified. Representative pictures were taken using an IX81 Olympus Spinning Confocal microscope images captured with a Hamamatsu Orca-ER Digital camera with a DSU spinning confocal unit and analysis using CellSens software.

Statistical Analysis

Prism software was used to perform all statistical analyses. All results are expressed as mean ± SEM. The significance of differences between two sample means was determined by Student's *t* tests using 95% confidence intervals. A p value less than 0.05 were considered significant.

Bibliography

Akhtar N, Streuli CH. An integrin-ILK-microtubule network orients cell polarity and lumen formation in glandular epithelium. Nat Cell Biol. 2013; 15:17–27. [PubMed: 23263281]

Akiyama SK, Yamada SS, Chen WT, Yamada KM. Analysis of fibronectin receptor function with monoclonal antibodies: roles in cell adhesion, migration, matrix assembly, and cytoskeletal organization. J Cell Biol. 1989; 109:863–75. [PubMed: 2527241]

Bonnans C, Chou J, Werb Z. Remodelling the extracellular matrix in development and disease. Nat Rev Mol Cell Biol. 2014; 15:786–801. [PubMed: 25415508]

Bryant DM, Roignot J, Datta A, Overeem AW, Kim M, Yu W, Peng X, Eastburn DJ, Ewald AJ, Werb Z, Mostov KE. A molecular switch for the orientation of epithelial cell polarization. Dev Cell. 2014; 31:171–87. [PubMed: 25307480]

Cardoso WV. Molecular regulation of lung development. Annu Rev Physiol. 2001; 63:471–94. [PubMed: 11181964]

Cardoso WV, Lu J. Regulation of early lung morphogenesis: questions, facts and controversies. Development. 2006; 133:1611–24. [PubMed: 16613830]

Chen WT, Chen JM, Mueller SC. Coupled expression and colocalization of 140K cell adhesion molecules, fibronectin, and laminin during morphogenesis and cytodifferentiation of chick lung cells. J Cell Biol. 1986; 103:1073–90. [PubMed: 3528168]

Danen EH, Sonneveld P, Brakebusch C, Fassler R, Sonnenberg A. The fibronectin-binding integrins alpha5beta1 and alphavbeta3 differentially modulate RhoA-GTP loading, organization of cell matrix adhesions, and fibronectin fibrillogenesis. J Cell Biol. 2002; 159:1071–86. [PubMed: 12486108]

Davis GE, Cleaver OB. Outside in: inversion of cell polarity controls epithelial lumen formation. Dev Cell. 2014; 31:140–2. [PubMed: 25373773]

Debnath J, Mills KR, Collins NL, Reginato MJ, Muthuswamy SK, Brugge JS. The role of apoptosis in creating and maintaining luminal space within normal and oncogene-expressing mammary acini. Cell. 2002; 111:29–40. [PubMed: 12372298]

Foty RA, Forgacs G, Pfleger CM, Steinberg MS. Liquid properties of embryonic tissues: Measurement of interfacial tensions. Phys Rev Lett. 1994; 72:2298–2301. [PubMed: 10055839]

Foty RA, Pfleger CM, Forgacs G, Steinberg MS. Surface tensions of embryonic tissues predict their mutual envelopment behavior. Development. 1996; 122:1611–20. [PubMed: 8625847]

Foty RA, Steinberg MS. The differential adhesion hypothesis: a direct evaluation. Dev Biol. 2005; 278:255–63. [PubMed: 15649477]

Francis SE, Goh KL, Hodivala-Dilke K, Bader BL, Stark M, Davidson D, Hynes RO. Central roles of alpha5beta1 integrin and fibronectin in vascular development in mouse embryos and embryoid bodies. Arterioscler Thromb Vasc Biol. 2002; 22:927–33. [PubMed: 12067900]

Fukuda T, Yoshida N, Kataoka Y, Manabe R, Mizuno-Horikawa Y, Sato M, Kuriyama K, Yasui N, Sekiguchi K. Mice lacking the EDB segment of fibronectin develop normally but exhibit reduced cell growth and fibronectin matrix assembly in vitro. Cancer Res. 2002; 62:5603–10. [PubMed: 12359774]

Huveneers S, Truong H, Fassler R, Sonnenberg A, Danen EH. Binding of soluble fibronectin to integrin alpha5 beta1 - link to focal adhesion redistribution and contractile shape. J Cell Sci. 2008; 121:2452–62. [PubMed: 18611961]

Hynes, RO. Fibronectins. New York: Springer-Verlag; 1990.

Hynes RO. A reevaluation of integrins as regulators of angiogenesis. Nat Med. 2002; 8:918–21. [PubMed: 12205444]

Itoh M, Nelson CM, Myers CA, Bissell MJ. Rap1 integrates tissue polarity, lumen formation, and tumorigenic potential in human breast epithelial cells. Cancer Res. 2007; 67:4759–66. [PubMed: 17510404]

Kraft S, Klemis V, Sens C, Lenhard T, Jacobi C, Samstag Y, Wabnitz G, Kirschfink M, Wallich R, Hansch GM, Nakchbandi IA. Identification and characterization of a unique role for EDB fibronectin in phagocytosis. J Mol Med (Berl). 2016; 94:567–81. [PubMed: 26637426]

Legate KR, Wickstrom SA, Fassler R. Genetic and cell biological analysis of integrin outside-in signaling. Genes Dev. 2009; 23:397–418. [PubMed: 19240129]

Mao Y, Schwarzbauer JE. Fibronectin fibrillogenesis, a cell-mediated matrix assembly process. Matrix Biol. 2005; 24:389–99. [PubMed: 16061370]

O'Brien LE, Jou TS, Pollack AL, Zhang Q, Hansen SH, Yurchenco P, Mostov KE. Rac1 orientates epithelial apical polarity through effects on basolateral laminin assembly. Nat Cell Biol. 2001; 3:831–8. [PubMed: 11533663]

Plosa EJ, Young LR, Gulleman PM, Polosukhin VV, Zaynagetdinov R, Benjamin JT, Im AM, VAN DER Meer R, Gleaves LA, Bulus N, Han W, Prince LS, Blackwell TS, Zent R. Epithelial beta1 integrin is required for lung branching morphogenesis and alveolarization. Development. 2014; 141:4751–62. [PubMed: 25395457]

Robinson EE, Foty RA, Corbett SA. Fibronectin matrix assembly regulates alpha5beta1-mediated cell cohesion. Mol Biol Cell. 2004; 15:973–81. [PubMed: 14718567]

Robinson EE, Zazzali KM, Corbett SA, Foty RA. Alpha5beta1 integrin mediates strong tissue cohesion. J Cell Sci. 2003; 116:377–86. [PubMed: 12482923]

Roman J, Mcdonald JA. Expression of fibronectin, the integrin alpha 5, and alpha-smooth muscle actin in heart and lung development. Am J Respir Cell Mol Biol. 1992; 6:472–80. [PubMed: 1533775]

Sakai T, Larsen M, Yamada KM. Fibronectin requirement in branching morphogenesis. Nature. 2003; 423:876–81. [PubMed: 12815434]

Schnapp LM, Hatch N, Ramos DM, Klimanskaya IV, Sheppard D, Pytela R. The human integrin alpha 8 beta 1 functions as a receptor for tenascin, fibronectin, and vitronectin. J Biol Chem. 1995; 270:23196–202. [PubMed: 7559467]

Schuger L. Laminins in lung development. Exp Lung Res. 1997; 23:119–29. [PubMed: 9088922]

Schuger L, Varani J, Killen PD, Skubitz AP, Gilbride K. Laminin expression in the mouse lung increases with development and stimulates spontaneous organotypic rearrangement of mixed lung cells. Dev Dyn. 1992; 195:43–54. [PubMed: 1292752]

Schwarz MA, Zheng H, Legan S, Foty RA. Lung self-assembly is modulated by tissue surface tensions. Am J Respir Cell Mol Biol. 2011; 44:682–91. [PubMed: 20616358]

Snyder JM, O'Brien JA, Rodgers HF. Localization and accumulation of fibronectin in rabbit fetal lung tissue. Differentiation. 1987; 34:32–9. [PubMed: 3301486]

Steinberg MS. On the Mechanism of Tissue Reconstruction by Dissociated Cells, Iii. Free Energy Relations and the Reorganization of Fused, Heteronomic Tissue Fragments. Proc Natl Acad Sci U S A. 1962; 48:1769–76. [PubMed: 16591009]

Takahashi S, Leiss M, Moser M, Ohashi T, Kitao T, Heckmann D, Pfeifer A, Kessler H, Takagi J, Erickson HP, Fassler R. The RGD motif in fibronectin is essential for development but dispensable for fibril assembly. J Cell Biol. 2007; 178:167–78. [PubMed: 17591922]

Taverna D, Hynes RO. Reduced blood vessel formation and tumor growth in alpha5-integrin-negative teratocarcinomas and embryoid bodies. Cancer Res. 2001; 61:5255–61. [PubMed: 11431367]

Wan HT, Mruk DD, Li SY, Mok KW, Lee WM, Wong CK, Cheng CY. p-FAK-Tyr(397) regulates spermatid adhesion in the rat testis via its effects on F-actin organization at the ectoplasmic specialization. Am J Physiol Endocrinol Metab. 2013; 305:E687–99. [PubMed: 23880313]

Warburton D, Lee MK. Current concepts on lung development. Curr Opin Pediatr. 1999; 11:188–92. [PubMed: 10349094]

White ES, Muro AF. Fibronectin splice variants: understanding their multiple roles in health and disease using engineered mouse models. IUBMB Life. 2011; 63:538–46. [PubMed: 21698758]

Wierzbicka-Patynowski I, Schwarzbauer JE. The ins and outs of fibronectin matrix assembly. J Cell Sci. 2003; 116:3269–76. [PubMed: 12857786]

Yang JT, Rayburn H, Hynes RO. Embryonic mesodermal defects in alpha 5 integrin-deficient mice. Development. 1993; 119:1093–105. [PubMed: 7508365]

Yu W, Datta A, Leroy P, O'Brien LE, Mak G, Jou TS, Matlin KS, Mostov KE, Zegers MM. Beta1-integrin orients epithelial polarity via Rac1 and laminin. Mol Biol Cell. 2005; 16:433–45. [PubMed: 15574881]

Yu W, Fang X, Ewald A, Wong K, Hunt CA, Werb Z, Matthay MA, Mostov K. Formation of cysts by alveolar type II cells in three-dimensional culture reveals a novel mechanism for epithelial morphogenesis. Mol Biol Cell. 2007; 18:1693–700. [PubMed: 17332496]

Abbreviations

ECM	extracellular matrix
EMAP II	Endothelial Monocyte-Activating Polypeptide II
FN	Fibronectin
HD	Hanging Drops
PODXL	Podocalyxin
SPC	surfactant protein C
3D-	Three-dimensional

Key Findings

1. Murine embryonic lung cells self-assemble into three-dimensional pulmonary bodies that are dependent on α5β1 integrin mediated fibrillogenesis for cell-cell mediated self-assembly - compaction and epithelial cyst formation.

2. Fibrillogenesis mediated by αV integrin is not sufficient to normalize epithelial cyst formation.

3. Loss of α5 integrin-mediated fibrillogenesis perturbed the ability of clustered epithelial cells to establish clear polarity, loss of epithelial cell pyramidal shape, and disrupted apical F-actin-rich deposition.

4. Lung epithelial cyst formation in the developing lung is mediated in part by α5β1 integrin dependent fibrillogenesis.
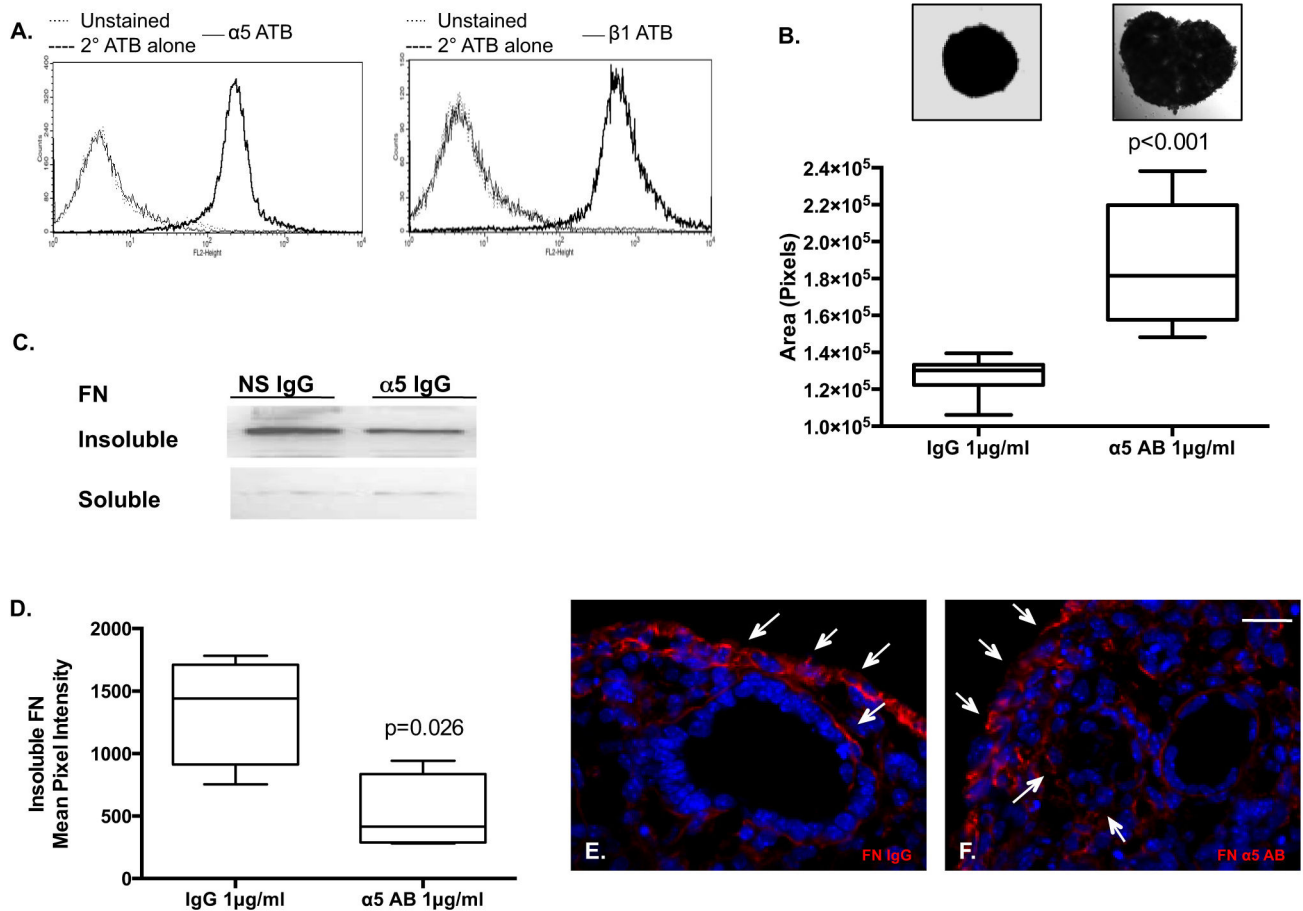
Figure 1. Fetal lung cells express surface antigens α5 and β1 integrins while neutralizing α5 integrin antibody reduces fibrillogenesis and compaction

Flow cytometry analysis at 488nm wavelength of dissociated embryologic day 14.5 lungs cell demonstrate surface expression of α5 and β1 integrin as compared to unstained and secondary Alexa - 488 antibody alone (A). The self-assembly or compaction of pulmonary cells into an aggregate in 3D hanging drops, pulmonary sheets, was assessed at 48 hours (measured as pixels). Pulmonary sheets treated with an α5-neutralizing antibody exhibited a less compaction measured as surface area in pixels ($1.862 \times 10^5 \pm 3.113 \times 10^3$ SEM pixels) as compared to non-specific IgG ($1.27 \times 10^5 \pm 9.344 \times 10^3$ SEM pixels) (B) (p<0.001) (unpaired Student's *t*-test, n=10/condition/experiment performed at least 5 occasions). Western Blot analysis of insoluble DOC FN (p=0.026, n=4, pooled samples, 4 different occasions) (C,D) and representative image of immunofluorescent FN indicated that coordinated long strands of insoluble FN are found in non-specific IgG pulmonary sheets (arrows, E) as compared to short thick FN depositions in α5 antibody (arrows, F) all supporting neutralization of α5 integrin mediated FN deposition. DAPI denotes nuclei. Scale bar: E,F = 20μm.

A.

B.

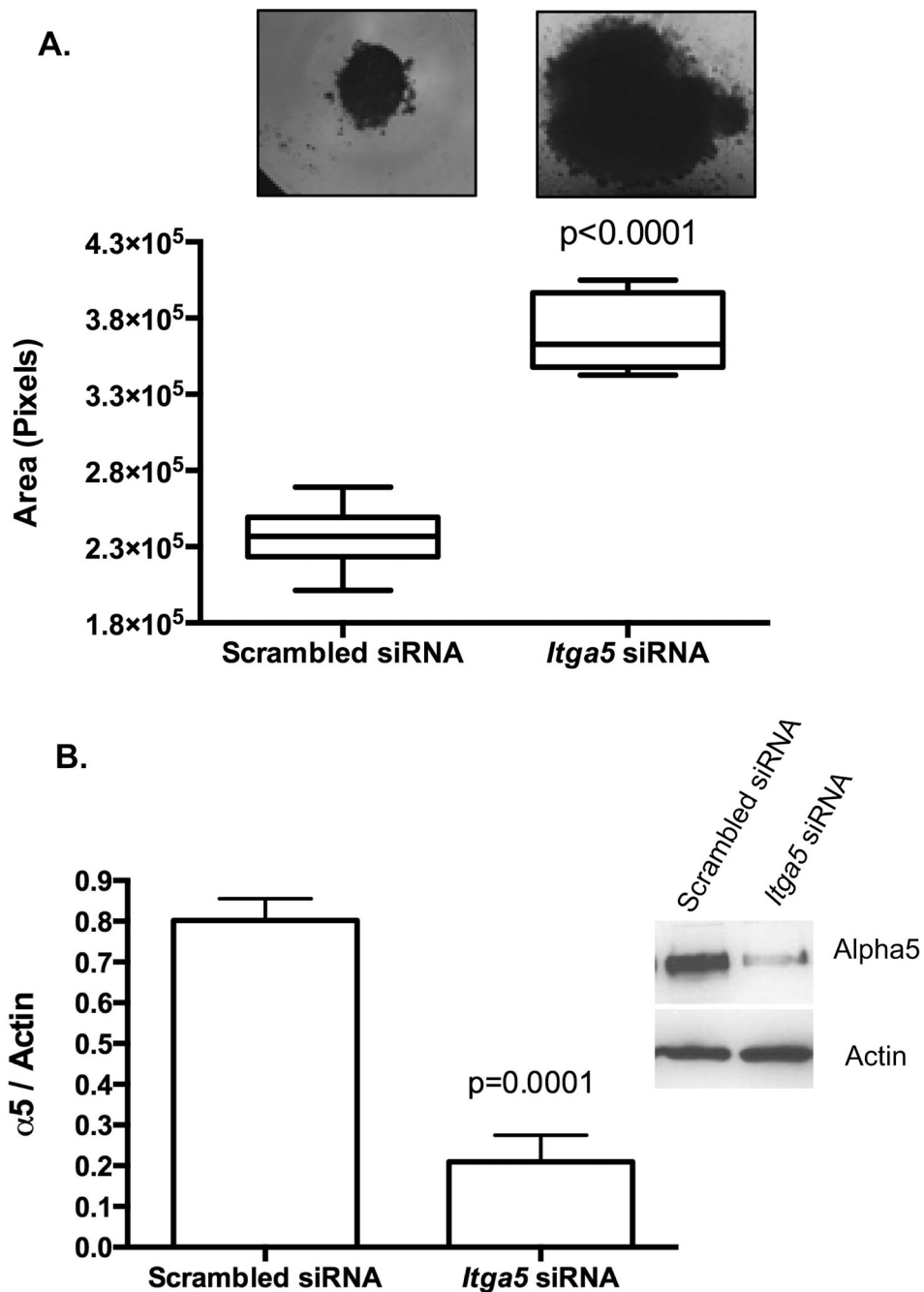**Figure 2. Knockdown of α5 integrin retarded pulmonary sheet compaction**
Dissociated fetal lung cells were reverse transfected with *Itga5* siRNA prior to being placed
in 3D hanging drops. The compaction or assembly of the dissociated 3D fetal lung cells
reverse transfected with *Itga5* siRNA into an aggregate within 48 hours noted as a
pulmonary sheet was assessed as compaction. HDs with knockdown of α5 exhibited
retardation in the amount of compaction ($2.36078 \times 10^5 \pm 6.576 \times 10^3$ SEM pixels) (A) as
compared to scrambled Scrambled siRNA ($3.70728 \times 10^5 \pm 7.697 \times 10^3$ SEM pixels,
p<0.0001, unpaired Student's *t*-test, n=10/condition/experiment performed at least 8 times).
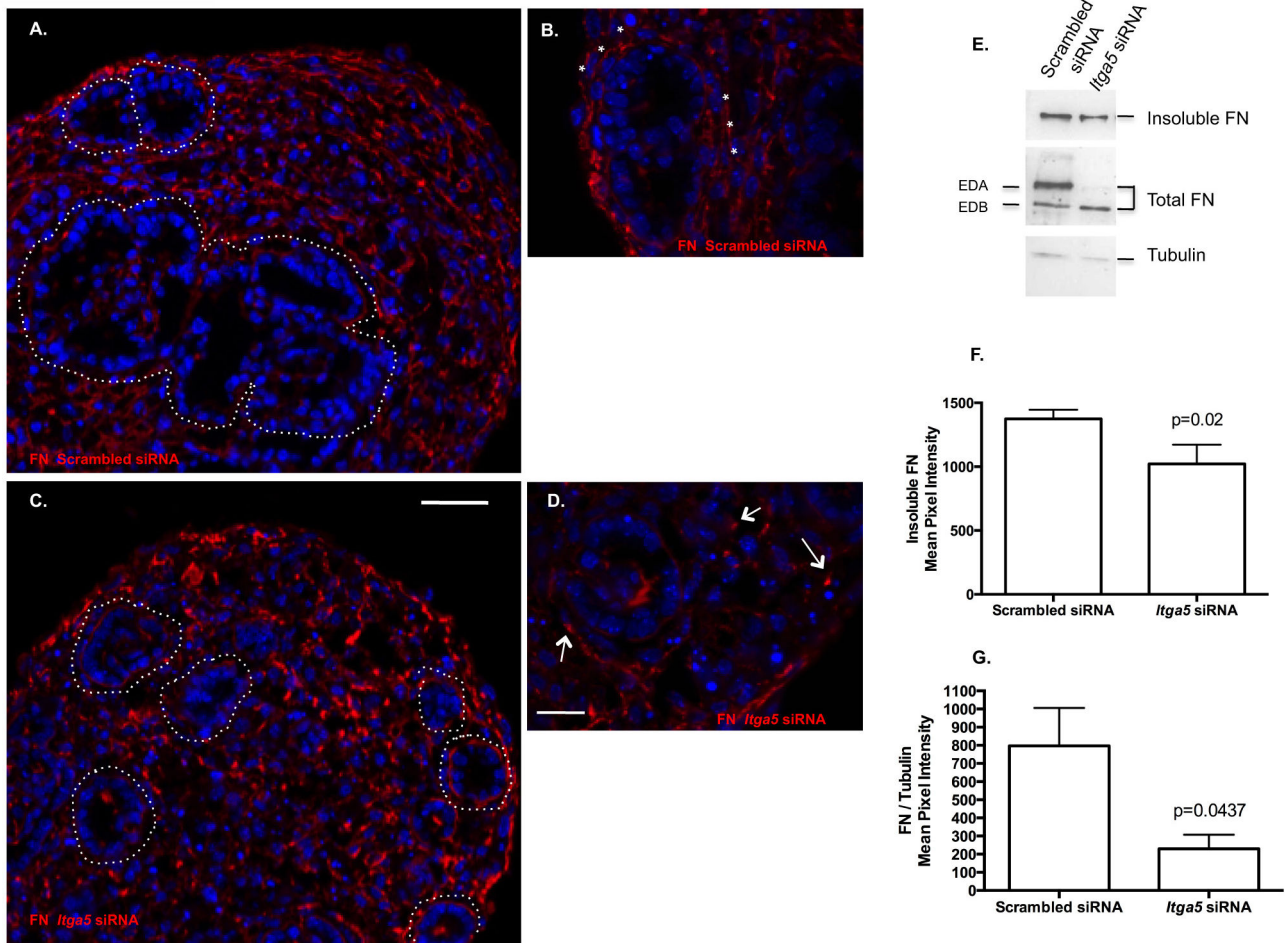
Western blot analysis of assessed pulmonary sheets supports a significant 74% reduction in α5 protein (B)(0.2094 ± 0.065 SEM mean pixel intensity) as compared to Scrambled siRNA (0.8020 ± 0.053 SEM mean pixel intensity) (p=0.0001, unpaired Student t-test, n=5, pooled samples from 5 different occasions).

Figure 3. *Itga5* siRNA disrupts FN matrix assembly

Fibrillogenesis occurs in HDs noted by deposition of insoluble FN in long strands within the HD (Fig. 3B: stars) as well as at the epithelial/mesenchymal interface (Fig. 3A: dotted outline) (IF, Cy3). Fibrillogenesis was suppressed by *Itga5* siRNA as noted by reduction of insoluble FN strands at the epithelial/mesenchymal interface by IF (C,D Cy3) (C: dotted white lines), presence of short, thick, arrowhead like FN punctata (arrow, D), Western blot analysis of isolated DOC insoluble FN (C-G) (1022 ± 149 SEM mean pixel intensity) (p=0.02, paired Student t test, n=5 pooled samples from different occasions), and total FN (E,G) (229.3 ± 77.92 SEM mean pixel intensity) (p=0.044, Students t test, n=5 pooled samples from different occasions) as compared to Scrambled siRNA (1374 ± 70 SEM mean pixel intensity and 797 ± 208 SEM mean pixel intensity respectively) (A: dotted white lines, B: *** long thin FN fibrils, E-G). Total FN demonstrated marked reduction in the alternative splice variants Extra domains A (EDA) in the *Itga5* siRNA while the Extra Domains B (EDB) was unaffected as compared to Scrambled siRNA (E). DAPI denotes nuclei. Scale bar: A,C=60µm and B,D=20µm.
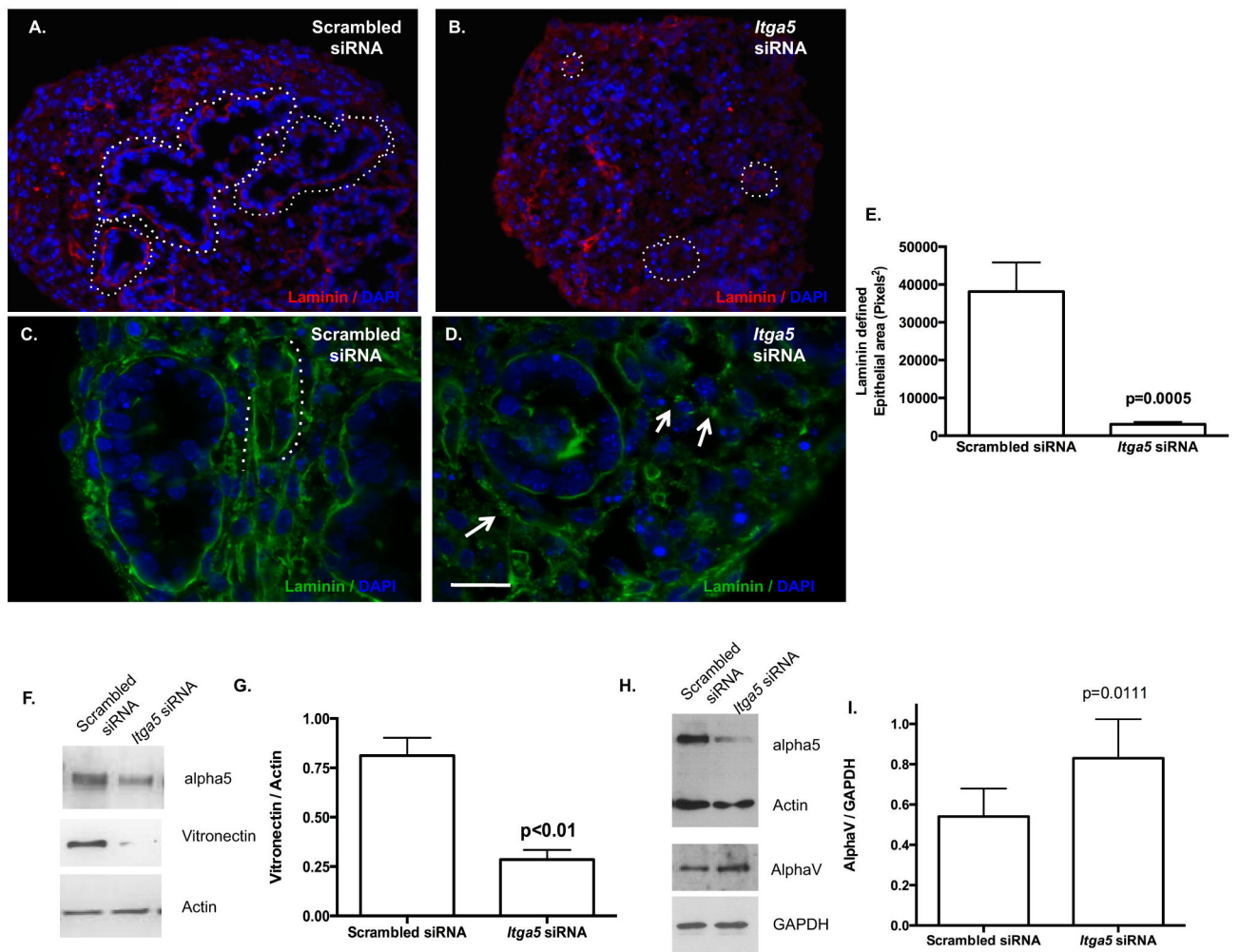
Figure 4. *Itga5* siRNA influences ECM basement membrane protein expression and deposition while impacting epithelial cyst formation

Long continuous laminin strands are noted in Scrambled siRNA (low magnification-A:Cy3 that is better appreciated at high magnification-C Alexa:488 – stars outline continuous laminin distribution). In contrast, laminin deposition was irregular in *Itga5* siRNA (B: low magnification, D: high magnification, white arrows demonstrated altered deposition). Epithelial lumen diameter, defined by its basement membrane laminin border is significantly reduced in *Itga5* siRNA HDs (B- white dotted outline of laminin epithelial lumens, E) (3,027 ± 616 SEM pixels, n=9, performed on a minimum of 2 different occasions, unpaired Student t test) as compared to Scrambled siRNA (38,140 ± 7,730 SEM pixels, A- white dotted outline of laminin epithelial lumens, E). Vitronectin protein expression was significantly suppressed (F,G, 0.5867±0.188 SEM mean pixel intensity) ($p<0.01$, paired Student t test, n=4 pooled samples from 4 different occasions) while Alpha V integrin protein expression was significantly increased (H,I, 0.8300±0.190 SEM mean pixel intensity) ($p=0.0111$, paired Student t test, n=6, pooled samples from 6 different occasions) in *Itga5* siRNA HD as compared to Scrambled siRNA (1.045±0.161 SEM and 0.5400±0.137 SEM respectively). DAPI denotes nuclei. Scale bar: A,B=60μm and C,D = 20μm.
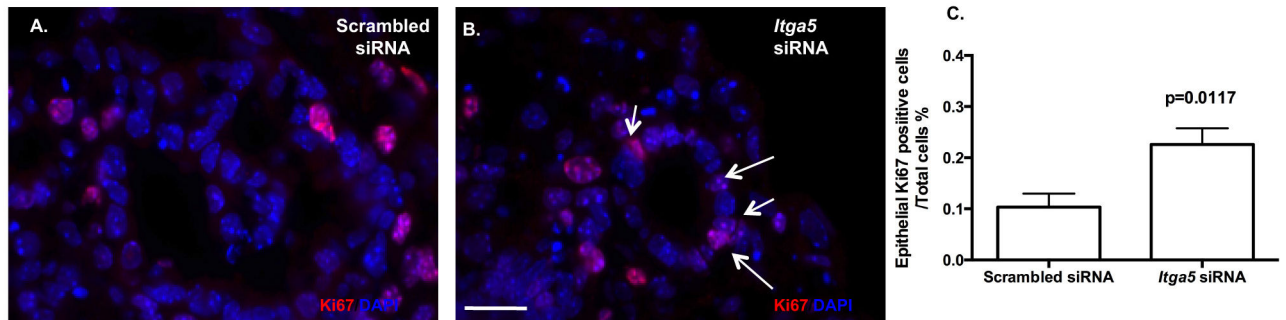
Figure 5. Alpha5 mediates lumen epithelial cell proliferation
Proliferation determined by Ki67 (cy3) and DAPI staining was increased in *Itga5* siRNA HDs in epithelial cells (B,C, 22.5% ± 3.1% SEM, n=7, samples from different occasions, unpaired Student t test) as compared to Scrambled siRNA (A,C, 10.36% ± 2.6% SEM respectively). Scale bar: A,B =20µm.
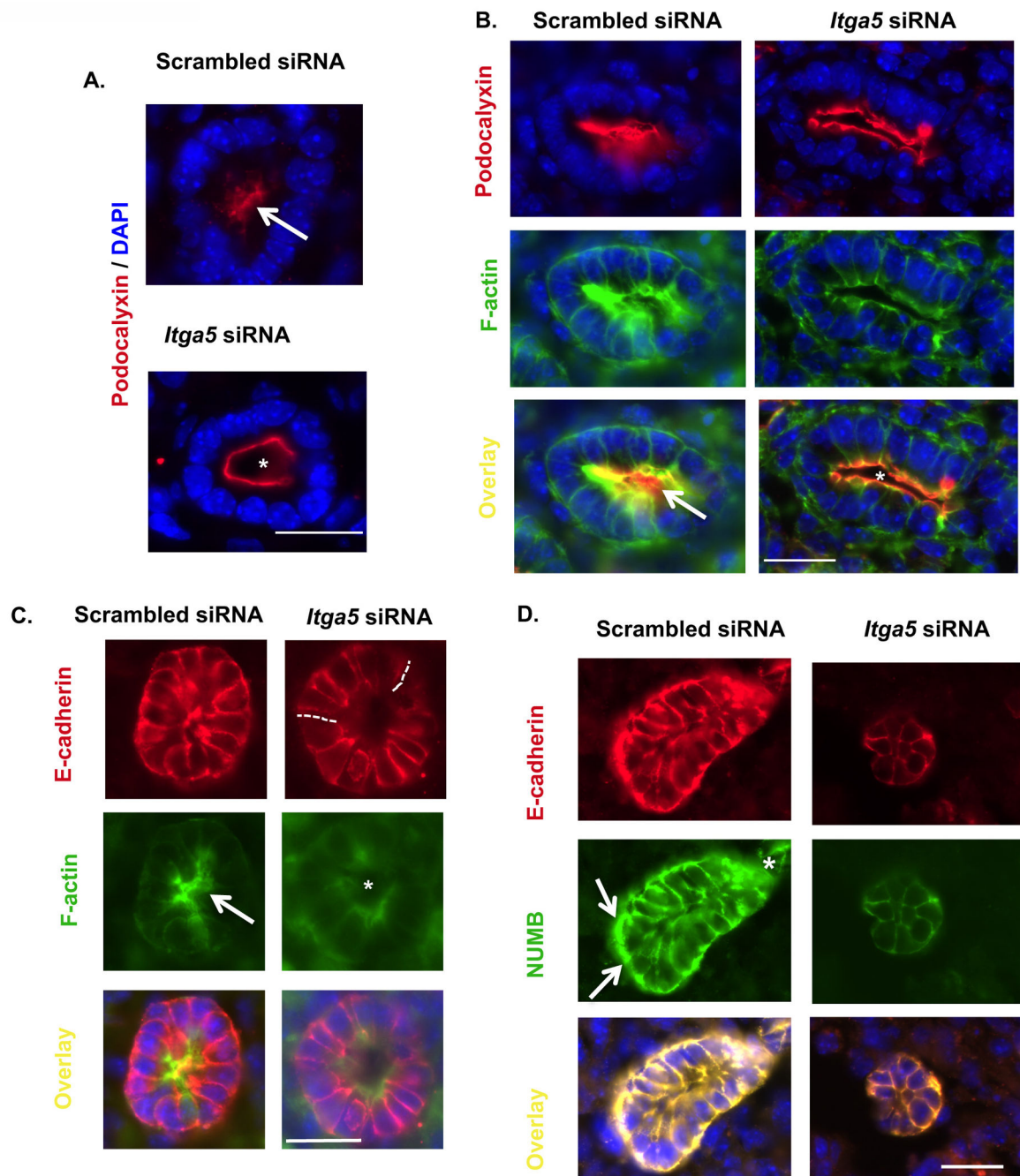
Figure 6. Alpha5 mediates epithelial front-rear and apical-basolateral polarity
Central Podocalyxin (cy3) epithelial lumen expression consistent with established epithelial apical-basolateral polarity in Scrambled siRNA HDs, was not central in *Itga5* siRNA HDs lumens (A-arrow normal epithelial apical deposition of podocalyxin, * indicates lack of central Podocalyxin). F-actin-rich central (B-AlexaFluor 488) epithelial lumen distribution is parallel that of Poldocalyxin with its central deposition supporting an apical-basolateral lumen polarity in scrambled siRNA HDs (B-arrow) compared to central F-actin-poor expression in *Itga5* siRNA (B, *). Adherens junctions in the epithelial lumens of *Itga5*

siRNA showed discontinuous E-cadherin at contact points (dotted lines-C, Cy3), columnar shaped epithelial cells and consistent apical epithelial F-actin-poor (C-AlexaFluor 488, *) as compared to central F-Actin-rich, pyramidal shaped epithelial cells, and continuous E-cadherin Scrambled siRNA (C). Epithelial cyst polarity in closed epithelial cyst using the marker NUMB and adherens junction marker E-cadherin demonstrated that front-rear polarity is found in Scrambled siRNA cyst with focal posterior NUMB deposition (D-strong rear expression: arrows) and limited distal expression (D-decreased front expression *) in Scrambled siRNA cyst while NUMB and E-cadherin distribution in closed *Itga5* siRNA epithelial cyst did not demonstrate obvious front-rear epithelial distribution (D). DAPI denotes nuclei. Scale bar: A-E= 20μm